Online spectral unmixing in gamma-ray spectrometry

Paul Malfrait, Jérôme Bobin, Anne de Vismes Ott

Online spectral unmixing in gamma-ray spectrometry

Paul Malfrait[a], Jérôme Bobin[b], Anne de Vismes Ott[a,*]

[a] *Institut de Radioprotection et de Sûreté Nucléaire (IRSN), PSE-ENV/SAME/LMRE, F-91400 Orsay, France*
[b] *CEA IRFU/DEDIP, 91191 Gif-sur-Yvette, France*

Abstract

We introduced in a previous paper a time-dependent full-spectrum analysis algorithm speeding up the estimation of the activity of the radionuclides present in a sample. In this paper, we present a new version of the algorithm allowing online estimation. It uses only on a buffer of few segments while keeping the time information by using a time dependent regularization, thus reducing the size of the data matrices and the length of the processing of each iteration. The algorithm is optimized and tested on both simulated and measured spectra of aerosol samples.

Keywords: gamma-ray spectrometry, model, full spectrum analysis, Poisson statistics-based spectral unmixing, metrological analysis

1. Introduction

In the context of radiological surveillance and radioecology studies, the analysis by gamma-ray spectrometry of aerosol filter samples allows to detect radionuclides at very low level (lower than 1 µBq/m^3 in the air *ie* less than 1 Bq per sample) that are present in the environment among large concentrations of natural radionuclides. The rapid analysis of a gamma-ray spectrum as it is produced is a challenge in gamma-ray spectrometry as the measurement process can be quite long (varying from 1 to 4 days). In fact, if one wants to analyse the spectrum in the minutes after the aerosol filter is sampled the gamma

*Corresponding author
Email address: anne.de-vismes@irsn.fr (Anne de Vismes Ott)

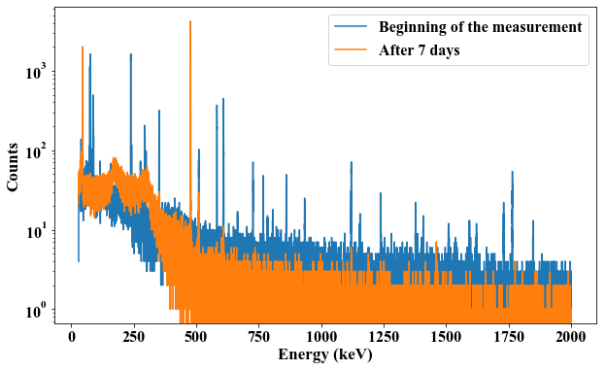

Figure 1: The spectrum obtained at the beginning of the measurement (first 20 minutes after the aerosol filter has been sampled) and the end of the week of measurement (last 4 hours). The two spectra contain the same number of counts.

ray spectrum is dominated by the radon progenies that are short-lived radionuclides. The routine method to analyse gamma ray spectrum, which generally relies on peak-based analysis, struggles to cope with the complexity of such spectra. For a precise analysis of low-level radionuclides, activity estimation is generally performed at least one day after the filter has been sampled. This is illustrated in figure 1, the blue signal is the spectrum of an aerosol filter sample time-integrated over the first 20 minutes after it has been sampled, it presents a lot of peaks, mainly due to radon progeny. The orange spectrum is the one of the same sample for a 4 hours long measurement after a week of decay.

This highlights that postponing the measurement long after the filter is sampled allows for a more accurate analysis of low-level long-lived radionuclides. However, estimating the activity of the radionuclides composing the spectrum as soon as possible is key in the context of radiation protection and emergency preparedness, and we will illustrate later in this article that the observed delay before measuring the samples and getting the first activity estimations can be problematic in case of air contamination.

The method introduced in this this paper is quite general. We will however focus on the OPERA-Air network aerosol filter measurement as it is done in the Environment Radioactivity Metrology Laboratory (IRSN/LMRE) and produces

gamma ray spectra that contain a high complexity due to the radon progeny.

1.1. State of the art

Quite formally, a gamma-ray spectrum is the histogram of the energy deposited by photons in the detector. The spectrum can be decomposed in various components that originate from each radionuclide contained in the measured sample. The contribution of each radionuclide is composed of sequence of energy peaks and their associated Compton continua (see Gilmore (2001) or Knoll (2010)). The analysis of gamma ray spectrum can be seen as the analysis of these different components and the quantification of their contributions in the total spectrum gives the activities of each radionuclides. The rapid analysis of gamma-ray spectra is a difficult problem due to the potential complexity of the spectra and the low level of the radionuclides of interest compared to the background and/or other radionuclides. For example the concentration of ^{137}Cs in the air is lower than 1 µBq/m^3 while the ^{7}Be level is at thousands of Bq/m^3.

New methods to analyse the gamma ray spectra are shown to be valuable in the case of the radiation protection and environment surveillance where complex spectra are observed. In routine measurements the analysis is based on the peaks present in the spectrum thanks to Genie 2000 (see Mirion-Canberra (2016)) but this method cannot cope with low level of activities and a delay has to be observed before the measurement is done to let the radon progeny decay and vanish from the spectrum. Moreover this method uses an approximation of the Poisson noise inherent to the counting process and the exponential decay of the radionuclides leading to the gamma-ray spectra that is considered as gaussian, this particularly impacts low level activity estimation where the Poisson noise cannot be approximated by a gaussian noise. This peak based method has been generalized to account for the Poisson noise in Kirkpatrick and Young (2009), but despite of this improvement the complexity of the spectra and the possible overlapping of the components of the spectrum is still problematic in peak-based analysis.

Using the full-spectrum information allows reducing the measurement time

and gaining in sensitivity as proven in Hendriks et al. (2001). In André et al. (2020) a new method based on the full spectrum analysis is proposed to deal with complex spectra containing a lot of radionuclides. Following these works the method has been improved to include a model selection via a sparse algorithm that allows to choose in a list of possible nuclides the ones that contribute to the observed spectrum (see Xu et al. (2020), Xu et al. (2022a), Xu et al. (2022b)). In Malfrait et al. (2023) a new method is proposed to estimate the activities as the measurement is processed by adapting the gamma-ray spectrum model to temporal analysis allowing to get a quicker estimation of the activity of the radionuclide composing the spectrum.

In the last years, new developments were made in the field of gamma-ray spectrometry using Artificial Intelligence tools such as Convolutional Neural Networks (Turner et al. (2021), Chaouai et al. (2022)) or Generative Adversarial Networks (de Oliveira et al. (2023)). In these articles the focus is on the creation of a learning set of data via simulation and the performance assessment on detection of radionuclides in different conditions like the presence of shielding, in a complex or laboratory controlled environment. These new methods are easy to compute once the training is done, leading to online applications that are fast without more development. On the other hand, these algorithms are very sensitive to variations from the learning data sets to real measurements, for example if the presence of a shielding affects the observed spectra or for low statistics such as low activity or short measurements.

Contributions. In this article we propose a new algorithm that allows online estimation of the activities as the measurement of aerosol filter samples is done. Thus drastically reducing the time to correctly estimate the activity of the radionuclides composing the spectrum (1 min to detect a few Bq of activity). This new analysis is based on the full spectrum unmixing and the multiplicative update algorithm showed in Malfrait et al. (2023) with a few tweaks allowing to deal with large matrices of data.

Based on the previous work the aim is to generalize the algorithm to any

number of time segments and to get an estimation of the activities in the sample as soon as possible during the measurement process. To achieve this, we seek to reduce the size of the data matrices involved in the unmixing process and to reduce the number of iterations needed to converge.

The improvement to the algorithm presented in Malfrait et al. (2023) will be presented on simulations and on a real aerosol filter sample measured in our laboratory. The detection of a few Bq of ^{123}I in a filter sampled for 1 week and an air volume of 90 000 m^3 after only a minute of measurement is achieved thus proving the performances of the unmixing in the case of fast detection. For ^{137}Cs, which is hard to detect as its activity is at the level of the decision threshold in the French environment, the detection is achieved after one day and 12 hours, which is almost four times faster than previous results based on full spectrum analysis Xu et al. (2020).

2. Temporal spectral unmixing

As stated in the introduction, a gamma ray spectrum is an histogram of the deposited photons in C channels representing the different energies. Following André et al. (2020), it can be modelled as the linear combination of radionuclides spectral signatures. The content of each of the C channels of the spectrum can be written:

$$\forall c = 1, \cdots, C; \quad x_c = \sum_{n=1}^{N} \phi_{nc} w_n + \delta b_c, \tag{1}$$

$$y_c \sim Poisson(x_c) \tag{2}$$

The signal x_c is the model spectrum without the Poisson noise coming from the counting process of the detection and the exponential decay of the radionuclides : y is the measurement, ϕ is the matrix that contains the N signatures of each radionuclides in column. The vector w_n is composed of the weights of each of the radionuclides. The scalar δ is the duration of the measurement in seconds and b is the background spectrum per second , it is the spectrum obtained for a

1-second measurement on an empty detector, obtained by normalizing a weak long measurement. As we focus on laboratory measurements the background is considered stable through the entire measurement (see Appendix A for details on the experimental setup that provides the background stability). The mixing weights, w_n, are proportional to the activity of the radionuclides in the sample. In fact, the mixing weights can be split in two factors following the radioactive decay formula:

$$\begin{aligned} \forall n = 1, \cdot, N; w_n &= a_n(0)\psi_n && (3) \\ \psi_n &= \int_{t_0}^{t_1} e^{-\lambda_n t} dt && (4) \\ & && (5) \end{aligned}$$

w_n is the accumulated number of disintegrations obtained for a measurement from t_0 to t_1. $a_n(0)$ is the activity of the n-th radionuclide at $t = 0$, in the following, it will be noted a_n, it is the quantity of interest we want to estimate. λ_n is the decay constant of the n-th radionuclide.

Following Malfrait et al. (2023) the temporal model to explain the gamma-ray spectra obtained on consecutive time segments is the following :

$$\begin{aligned} X &= \Phi(\Psi diag(a)) + B \\ Y &\sim Poisson(X) \end{aligned} \tag{6}$$

With:

- $diag(a)$ being the matrix containing all the activities $(a_1, ..., a_N)$ of each radionuclides at time $t = 0$ on its diagonal and 0 outside of its diagonal.
- X a $C \times S$ matrix, it is the base gamma ray spectrum without the Poisson noise, where S is the number of time segments considered.
- Φ a $C \times N$ matrix composed of the spectral signatures of the radionuclides composing the spectrum. A spectral signature is the gamma ray spectrum

obtained with the measurement of an activity of 1 Bq for 1 s. It is the response of the detector with respect to the emission of a given radionuclide. These signatures can be obtained from the measurement of single radionuclide sources. However, these sources being hardly available for some radionuclides, they are generally derived from simulations. In this article, they have been simulated with MCNP-CP (see Berlizov (2012)), the details of the detector and the simulations can be found in Appendix A.

- Ψ a $N \times S$ matrix containing the temporal information. It is the integral of the radioactive decay model of the n-th radionuclide over each time segment:
$$\psi_{n,s} = \int_{t_s-1}^{t_s} e^{-\lambda_n t} dt$$
- B is a $C \times S$ matrix representing the background spectrum of the detector. This matrix can be decomposed into : $B = \delta.b$ where δ is the vector of the segment duration in second and b is the normalized background spectrum of the detector we use.
- Y is the Poisson-noised version of X, the Poisson noise comes from the counting process of the gamma-ray measurement.

In Malfrait et al. (2023), we introduced a time-dependent model for the full spectrum analysis of gamma ray spectra with a corresponding algorithmic scheme. We showed that accounting for the time dependency of consecutive measurement of the same aerosol filter sample fasten the estimation time, with reducing uncertainties as the data are collected in time. This was achieved by including the radioactive decay model in the spectral unmixing procedure. This way, activity estimation can be performed from multiple time measurements at once. Moreover, we showed that finely describing the decay chains could help in the estimation of low level radionuclides that would otherwise be slightly biased. In fact as we are dealing with the radon progeny before its decay we have to take into account multiple decay chains namely ^{214}Pb/^{214}Bi and ^{212}Pb/^{212}Bi/^{208}Tl.

In this article both chains are considered at equilibrium and each daughter radionuclides adopts the period of its parent. The detailed model in the case of out of equilibrium chains and Bateman equation is needed can be found in Malfrait et al. (2023).

The mathematical model presented in equation 6 allows to tackle the activity estimation of the radionuclides as an inverse problem that can be solved using the multiplicative update algorithm (see Lee and Seung (1999)).

While satisfactory on a small number of time segments (*e.g.* 11 consecutive measurements used in Malfrait et al. (2023)), applying this algorithm to a very large number of segments in an online estimation scheme is problematic as the data to be processed increase with time, and spectral unmixing has to be performed each time a new measurement is collected. A dedicated algorithm is needed to perform spectral unmixing using temporal correlations on a fine time sampling of the measurement.

2.1. Full spectrum analysis with time dependence

To account for the time decay of the radionuclides to perform time-dependent processing, a new algorithm has been introduced in Malfrait et al. (2023), it is an extension of the full-spectrum analysis method proposed in André et al. (2020). This algorithm is based on a multiplicative update scheme so that, at each iteration k to $k+1$, the activities of the radionuclides are updated simultaneously as follows:

$$a_{sn}^{(k+1)} = a_{sn}^{(k)} \frac{\sum_{c=1}^{C} \phi_{nc} y_{sc}/x_{sc}}{\sum_{c=1}^{M} \phi_{nc}}, \tag{7}$$

Where $Y_s = (y_{s1}, ..., y_{sC})$ is the observed spectrum during the s-th segment and $X_s = (x_{s1}, ..., x_{sC})$ is the theoretical model as viewed in equation 6. The multiplicative update is performed until convergence, which we define as :

$$\frac{\sum_n (a_n^{(k+1)} - a_n^{(k)})^2}{\sum_n {a_n^{(k)}}^2} \leq \epsilon_{diff} \tag{8}$$

ϵ_{diff} is usually taken small (10^{-6} in this paper).

This update allows us to minimise the following loss function in term of the activities:

$$L(\{y_{sc}\}_{s,c}|\{a_n\}_n) = \sum_{s,c} x_{sc} - y_{sc}\log(x_{sc}) + \log(y_{sc}!) \quad (9)$$

$$x_{s,c} = \sum_{n=1}^{N} \phi_{c,n}\psi_{n,s}a_n + \delta_s b \quad (10)$$

The algorithm thus aims at reducing the difference between the theoretical spectrum (X_s) and the observed one (Y_s) in terms of the Kullback-Leibler divergence (Kullback and Leibler (1951)).

The main aspects that we will focus on to reduce the computation time are : (i) reduce the number of iterations while keeping a correct estimation of the activities and (ii) reduce the size of the matrix involved in the update so that the computation can be done even with a really fine time segmentation and a huge data matrix.

2.2. Reducing the size of the data matrix involved at each iteration

The main limitation of the time-dependent algorithm introduced in Malfrait et al. (2023) is that, for s time segments, the size of the data matrix to be analysed is equal to $s \times C$. For a typical aerosol sample with about 16000 energy channels, jointly analysing a 100 time segments requires performing spectral unmixing on matrix with more than a million entries. This first requires a significantly important computational cost, and for a large number of time segments, an increasingly large matrix to be stored. In the context, both the data matrix X and temporal model matrix Ψ grow in size.

In order to make online time-dependent spectral unmixing tractable, the proposed approach consists in lowering the size to the matrix to be handled each time a new time segment needs to be processed. For that purpose, we chose to set a maximum size to the matrix and to process the data as a buffer of fixed size r. More precisely, the data matrix describing the observed spectra is :

$$\begin{pmatrix} | & | & ... & | \\ x_1 & x_2 & ... & x_s \\ | & | & ... & | \end{pmatrix}$$

The buffer we propose to use instead is :

$$\begin{pmatrix} | & | & ... & | \\ \sum_{k=1}^{s-r+1} x_k & x_{s-r+2} & ... & x_s \\ | & | & ... & | \end{pmatrix}$$

If we were to build a small size buffer from few past time segments, the resulting procedure would suffer from two main drawbacks:

- It would only account for the time decay of the radionuclides on a short duration, which would limit the efficiency of the unmixing process.
- For short-lived, the activity estimation procedure would become unstable as their activity would quickly vanish.

To mitigate these two pitfalls, we add to the buffer the sum of the past measurements from time segment 1 to $s - r + 1$. Formally, it will be stored in the first column of the buffer. This procedure allows limiting the instability of the activity estimation of the short-lived radionuclides. This is illustrated in figure 2: if only the segments x_{s-r+1} to x_s are used the activity estimation explodes due to the vanishing activity of the short-lived radionuclides.

2.3. Regularising the activity estimation in time

As we pointed out in the previous paragraph, performing spectral unmixing on a small size buffer allows avoiding manipulating large data matrices but at the cost of reducing the time interval on which time decay is exploited. From a statistical viewpoint, processing numerous short-duration time segment also entails that spectral unmixing will have to capture time-dependency from few time segments with potentially a low number of counts. This could also result

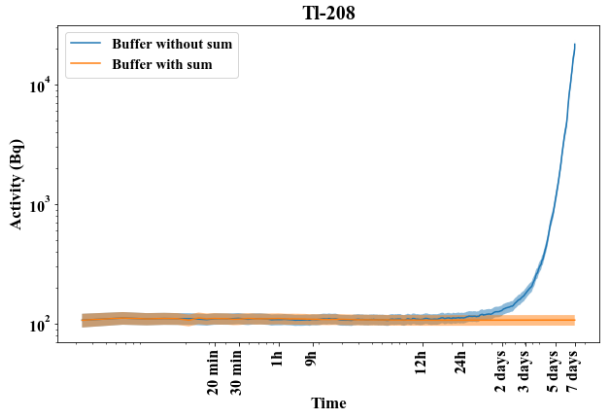

Figure 2: The activity estimation of ^{208}Tl with respect to the measurement time, which half life is 10.6h (because it is considered at equilibrium with ^{212}Pb)

in an unstable estimation of the activity in time.

To limit this source of instability, we propose to regularise the estimation of the radionuclides in time by imposing a time-dependent regularisation: loss function is altered so that the estimation of the activity for time segment s does not deviate too much from the last estimation produced at time $s-1$. In details, we add an extra term that limits some distance between the sought-after activity at time s and its previous value at time $s-1$. This results in the following loss function:

$$L(\{y_{sc}\}_{s,c}|\{a_n\}_n) = \sum_{s,c} x_{sc} - y_{sc}\log(x_{sc}) + \log(y_{sc}!) + \beta\ dist(a_{s-1}, a) \quad (11)$$

The distance $dist$ is chosen as the Kullback-Leibler divergence between the estimated spectrum at time $s-1$ and the estimated spectrum at time s this leads to:

$$dist(a_{s-1}, a) = \sum_{s,c} x_{sc} - x_{s-1,c}\log(x_{sc}) + \log(x_{s-1c}!)$$

where $x_{s-1,c} = \sum_{n=1}^{N} \phi_n \psi_{n,s} a_{s-1,n} + \delta_s b$ is the estimated spectrum using the $(s-1)$-th estimation of the activities.

As a consequence, this choice allows for a simple multiplicative update step that is similar to the one we implemented in the original time-dependent spectral unmixing algorithm.

The factor β is a regularisation parameter that controls the trade-off between the new information carried by the measurement at time s and the past value at time $s-1$. In fact, if we set $\beta = 0$, the weight given to the past estimation is zero and the update is the same as in Malfrait et al. (2023). This would lead to a less stable estimation of the radionuclides activity. If, on the other hand, β is too large, the estimation will remain almost stationary from one time step to another. This will affect the quality of the activity estimation since the estimation will poorly benefit from the long measurement process and will focus only on the first time segment. This would result in a very slow and biased estimation procedure.

The value of β needs to be optimised to get a good compromise between the speed of the algorithm to the correct activity and the stability of the estimation scheme in time. This will be detailed in section 3.

In order to make explicit the resulting multiplicative update scheme with the new regularised loss, we need to compute its derivative with respect to each a_n is:

$$\frac{\partial L(\{y_{sc}\}_{s,c}|\{a_n\}_n)}{\partial a_n} = \sum_{s,c}\left(\psi_{sn}\phi_{nc} - \frac{\psi_{sn}\phi_{nc}y_{sc}}{x_{sc}}\right) + \tag{12}$$

$$\beta\sum_{s,c}\left(\psi_{sn}\phi_{nc} - \frac{\psi_{sn}\phi_{nc}x_{(s-1)c}}{x_{sc}}\right) \tag{13}$$

where $x_{(s-1)c} = \psi_{sn}\phi_{nc}a_{(s-1)n} + b_{sc}$. To obtain the update rule we have to zero the derivative of this function with respect to each parameter as in Lee and Seung (1999). As the chosen quasi-distance is the Kullbach-Leibler divergence we can see that the structure of both terms in equation 13 are similar, leading to a compact update step that reads as :

$$a_n^{(k+1)} = a_n^{(k)} \frac{\sum_{s,c} \psi_{ns}\phi_{cn}.(y_{cs} + \beta x_{cs}^{(s-1)})/x_{sc}}{(1+\beta)\sum_{s,c} \psi_{ns}\phi_{cn}} \tag{14}$$

This new update step allows keeping the last activity estimation as a good starting point for the computation of the new one and forces the algorithm to converge quicker to a new estimation.

2.4. Updating only the radionuclides that are still active in the incoming data

A last source of instability could originate from the estimation of the short-lived radionuclides, when their activity becomes very low. In this case, keeping updating their activity is very likely to yield noise overfitting. To mitigate this effect, we propose adopting an early stopping procedure for short half-lives.
In fact, on a week-long measurement with some radionuclides that have short half-lives (*eg.* ^{214}Pb with a half-life of 26.8 min), their contribution to the spectrum tends quickly to 0. Adding new time measurements does not bring more information to update their activity. Moreover, updating their activity will tend to fit noise rather than actual physical contributions. Hence, we proposed adding a stopping rule to estimation procedure of the radionuclides's activity for which we know that there are no counts in the incoming spectrum.

This stopping rule is defined as follows : if the expected contribution of a radionuclide is less than a fixed number of counts (ϵ_{counts}), then the estimation is not updated. The expected number of counts is obtained through the following formula for any radionuclide n and any time segment s :

$$count_{n,s} = ||\phi_n||_1.\psi_{n,s}.\max(a_{n,s-1}, 1) \tag{15}$$

This way of computing the expected number of counts ensures that the radionuclides that have a very small activity (*eg.* ^{137}Cs) are still being updated even if the number of counts that are due to them is low while leaving the short-lived radionuclides out of the new estimation. Indeed, the contribution of these radionuclides can be small but they are still valuable, and we want to

estimate correctly their activities. Moreover, we will see in the next section (3) that the estimation of the radionuclides that have a low activity can be null if we analyse only the first time segments and increase as time goes, and more data are acquired.

This criterion allows us to focus only on the radionuclides that contribute to the new measured spectrum while keeping the estimation fixed for the radionuclides that do not contribute any more. This combined, with the stopping criterion of the algorithm (see 8), contributes to keep the number of iterations as low as possible as the number of coordinates of the activity estimation that are updated is low and thus the difference between the estimation at time $s-1$ and time s is null for some of them.

The different new tools that we developed are summarized in the following algorithm (1). If the buffer are used the matrices Ψ, Y and B are changed to the corresponding reduced matrices.

3. Numerical evaluation of the online spectral unmixing algorithm

In this section, we focus on evaluating the performances of the proposed online spectral unmixing algorithm on simulated data. We first start with the optimisation of the value of the regularisation parameter β, which plays a key role to balance between estimation bias, speed and stability.

Indeed, as we can see in table 1, we simulate spectra with very close activities to the one we observe on real aerosol filter samples. This way we can assess the performances of the unmixing algorithm on realistic simulations. The activity of the different radionuclides varies from really low levels (few mBq) to high activity (hundreds of Bq) as shown in table 1.

Thanks to the gamma-ray spectrum mathematical model (equation 6) we can simulate any mixture of signatures and apply a random Poisson noise to create realistic simulations of gamma-ray spectrum on which we apply our algorithm. The size of the buffer is fixed to 5 so that the computations are quick

Algorithm 1 The proposed unmixing algorithm

Require: $Y = (y_1, ..., y_s)$, $\Phi = (\phi_1, ..., \phi_N)$, $\Psi = (\psi_1, ..., \psi_s)$, $a_{s-1}, \epsilon_{count}$, ϵ_{diff}, $B = (\delta_1 b, ..., \delta_s b)$, β, K

$E = \emptyset$

$x^{s-1} \leftarrow \Phi(\Psi diag(a_{s-1})) + B$

$Diff \leftarrow \epsilon_{tol} + 1$

$\hat{a} = a_{s-1}$

$a = a_{s-1}$

for $i = 1, ..., N$ **do**

  $count \leftarrow ||\phi_i||_1 \psi_{is} max(a_{i,s-1}, 1)$

  if $count \geq \epsilon_{count}$ **then**

    $E \leftarrow E \cup \{i\}$

  end if

end for

$k = 0$

while $Diff \geq \epsilon_{diff}$ and $k \leq K$ **do**

  $k = k + 1$

  $x_s \leftarrow \Phi(\Psi diag(a)) + B$

  for i in E **do**

    $\hat{a}_i \leftarrow a_i \frac{\sum_{s,c} \psi_{ns} \phi_{cn} . (y_{cs} + \beta x_{cs}^{s-1}) / x_{sc}}{(1+\beta) \sum_{s,c} \psi_{ns} \phi_{cn}}$

  end for

  $Diff \leftarrow \frac{\sum_{n=1}^{N} (\hat{a}_n - a_n)^2}{\sum_{n=1}^{N} {a_n}^2}$

  for i in E **do**

    $a_i \leftarrow \hat{a}_i$

  end for

end while

return a

to perform and we can simulate a great number of Monte-Carlo repetitions for each experiments. An energy and efficiency calibration step are done to better simulate the detectors response to each of the radionuclide of interest (details

Radionuclide (subgroup)	Half-life	Simulated activity (Bq)	Estimated activity after 1 min (Bq)	Estimated activity after a week (Bq)
^{7}Be (i)	53.22 d	150	159 ± 29	157 ± 16
^{22}Na (ii)	2.60 y	0.02	0.49 ± 0.79	0.0284 ± 0.0033
^{40}K (ii)	1.265 10^{9} y	0.5	13 ± 10	0.511 ± 0.079
^{123}I (iii)	13.22 h	2	2.13 ± 0.71	2.48 ± 0.27
^{137}Cs (ii)	30.05 y	0.01	0.61 ± 0.66	0.0213 ± 0.0033
^{208}Tl (iii)	3.06 min	100	107 ± 14	107 ± 11
^{210}Pb (i)	22.3 y	30	30.0 ± 9.9	30.9 ± 3.2
^{212}Bi (iii)	60.54 min	300	339 ± 56	323 ± 33
^{212}Pb (iii)	10.64 h	200	237 ± 28	241 ± 24
^{214}Bi (iii)	19.9 min	300	328 ± 39	395 ± 42
^{214}Pb (iii)	26.8 min	100	114 ± 15	124 ± 14
^{228}Ac (ii)	14.02 10^{9} y	0.1	5.6 ± 2.6	0.132 ± 0.017

Table 1: The 12 simulated radionuclides, their subgroup, half-life and simulated activity. The estimated activities after 1 min and a week are presented for the real aerosol filter measurement with associated uncertainties (at k=2).

on the detector can be found in Appendix A or Paradis et al. (2017)).

3.1. Optimisation of the regularisation parameter β

In section 2, we highlighted that β is important to stabilise the activity estimation procedure in time as it controls how much the estimated activity at time s can deviate from its previous estimate.

The impact of β is twofold: i) a large value will tend to slow down the estimation in time and bias the estimates by giving too much weight to past time segments, and ii) a small value will tend to favor newest measurements in the activity

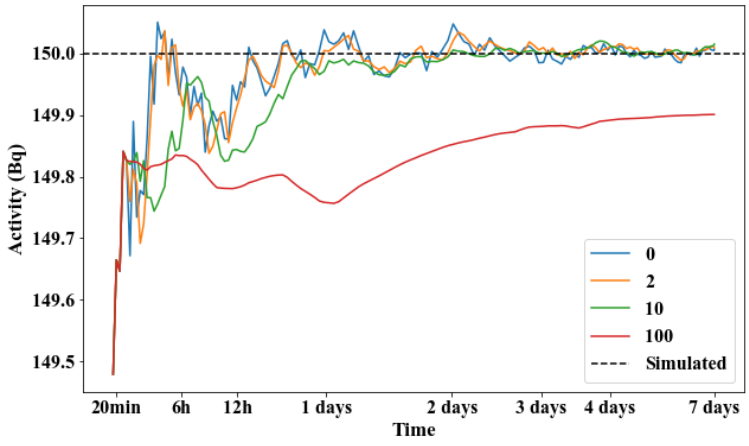

Figure 3: The median of the activity estimation of ^{7}Be with respect to the value of beta on 1000 Monte-Carlo simulations.

update step leading to potential instability.

The optimization of the value of β also allows us to assess the convergence and performances of the algorithm as a function of β. To choose an efficient trade-off for β, we performed simulations and found a good compromise between the correct estimation of the activities and a rapid convergence of the algorithm at each time step.

First, we can see in figure 3 the effect of the value of β on the estimation. As the value of β grows, so does the bias between the simulated activity and the estimation provided by the algorithm. Indeed, a large value of β implies that the update step only focuses on reducing the distance between the past estimation and the new one, the new estimation will then be equal or near the previous one. This is bad as the new information carried by the spectrum entering the analysis are not taken into account in the new estimation of the activities. As it can be observed in figure 3 the larger β is the larger the bias is at the end of the week-long measurement. For small values of β the effect is only to smooth the consecutive estimations, indeed the memory kept in the estimation leads the estimation at time s to be close to the new one at time $s+1$ while still allowing to converge to the correct estimation.

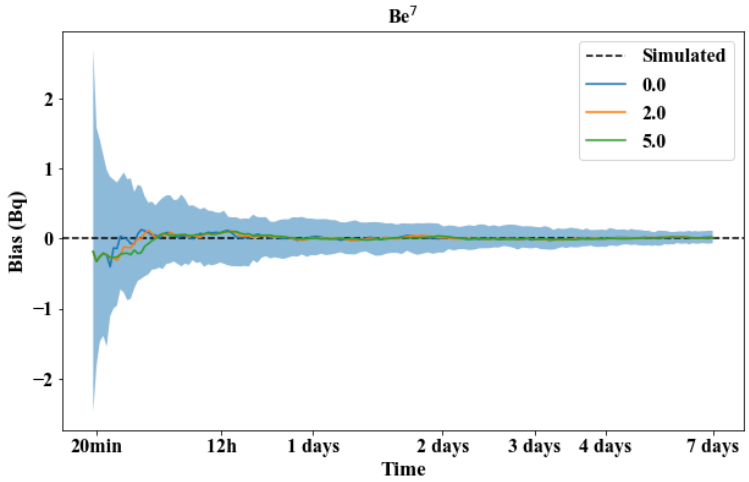

Figure 4: The bias on the activity estimation with respect to the value of β. We focus on small values of this parameter. The results are based on 1000 Monte-Carlo simulations.

After this first test we can focus on small values of β, the results of this second study are presented in figure 4. In this figure we can see that the bias of estimation does not vary a lot from one value of β to another as long as β is reasonably low (ie : $\beta \leq 2$). This allows to focus only on the computation time required to converge, indeed we want to find the smallest value of β that allows to reduce the computation time. The computation time will be seen as the number of iterations the algorithm needs at each time steps to converge (we recall that the stopping criteria is the distance between two consecutive iterations of the algorithm as viewed in equation 8).

Figure 5 displays the evolution of the computation time with respect to the value of β. One can observe that when the value of β increases, the computation time reduces. Indeed, the loss function requires the algorithm to remain near the estimation of the previous time segments and reduces the searching range to a vicinity of this past estimation. The higher the value of β the smaller the vicinity, thus reducing the number of iterations of each time step. The results of figure show that a good compromise between the convergence and the computation time is $\beta = 2$. In fact, increasing the value of β does not reduce

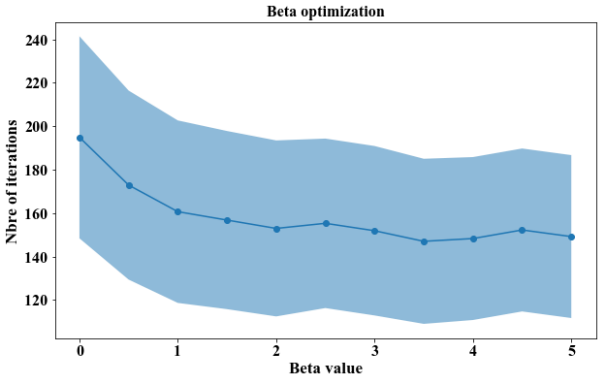

Figure 5: The mean number of iteration needed to converge (over the week of measurement) with respect to the value of β.

the computation time as much after $\beta = 2$. On the other hand, we have seen that allowing β to be high can create a significant bias on the estimation.

3.2. Performances of the unmixing algorithm

In this section, we further explore the simulations with $\beta = 2$ and the results of the estimation on high and low activities. The results of this section show the performances of the proposed online spectral unmixing algorithm to estimate the activity of 12 simulated radionuclides.

The radionuclides we simulate, and their activities are presented in table 1. We can split these radionuclides in three groups for analysis purposes : (i) the high activities with long half-life, (ii) low activity and long half-life, (iii) short half-life radionuclides. We focus on an example of each group (i) and (ii) and on two examples for group (iii) as it contains high and low activities. The results of our algorithm on simulations are shown in figure 6.

For the first group, an example of which is the ^{7}Be, the activity estimation is not difficult, the activity is high and the long period ensures a stable presence of the signature of these radionuclides in the spectrum. The correct estimation is achieved after only 2 minutes of measurement and can probably be even quicker (for computation time of the simulation we did not test the algorithm to a much finer segmentation than 2 minutes). The estimation of the activity

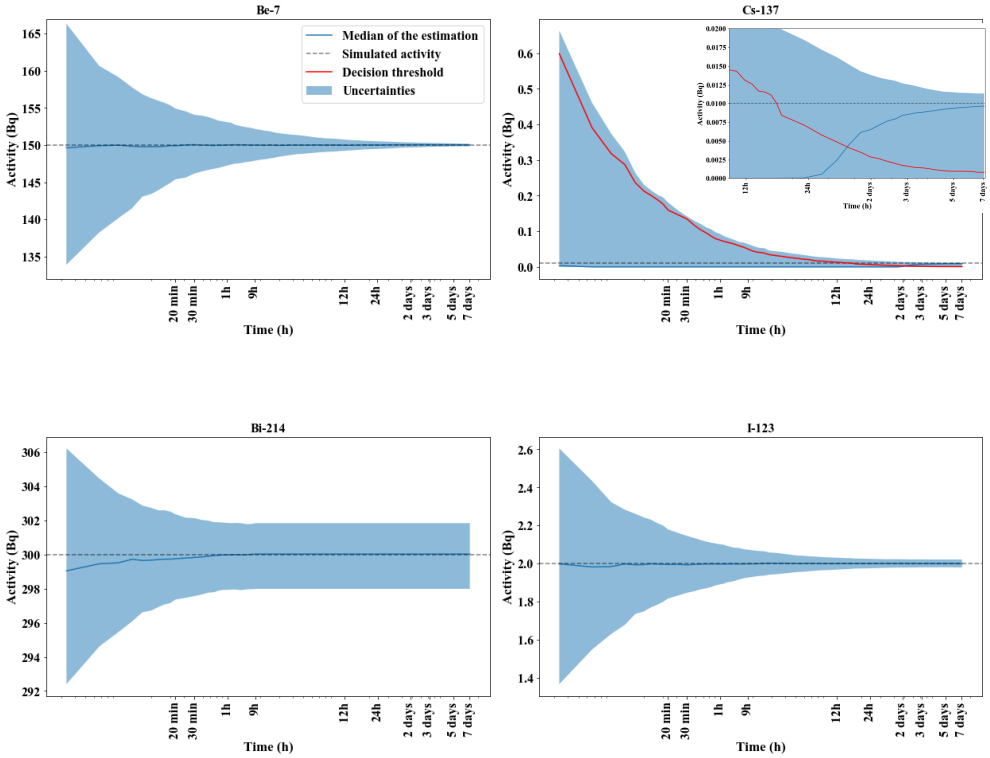

Figure 6: Results on simulations of the unmixing algorithm. The error bars are the 10% and 90% quantiles of the estimations based on 1000 Monte-Carlo simulations.

of the second group, such as ^{137}Cs, is much harder, in fact we observe activities that are close to the detection limit, the contribution of the radionuclides of this group to the spectrum is thus close to zero. The estimation can be null in the first segments and be achieved only after a short measurement time is observed. This is the case for ^{137}Cs, for which the detection limit is achieved only after 37h of measurement due to its really low simulated activity (0.01 Bq). For the radionuclides such as ^{123}I or ^{214}Bi, belonging to the third group, we note that the activity estimation is stable through time and is correct after only a few minutes. This shows the performances of the temporal unmixing to perform even for low level (1Bq of activity) radionuclides with short half-life (*eg* 13.22h in the case of ^{123}I). The stable performances for these short half-lived radionuclides are allowed thanks to the type of buffer that we adopted, that keeps track of the past time segments as previously seen in section 2.2. The other radionuclides' estimation behave the same as these examples depending on their activities and half-life.

Concerning the uncertainties, it is important to note that the main factor that impacts them is the half life of the radionuclides. In fact, if the period is short then the radionuclides contribution to the new time segments tends to 0, the uncertainty regarding its activity does not vary after this effect. On the other hands, for long-lived radionuclides the uncertainties decrease as long as the measurement is done and more and more statistics are taken into account. The uncertainties presented in this section only concern the statistical variability as the only random factor is the Poisson noise of the simulated spectra. The metrological uncertainties (around 10% of the estimated activity) must be added to this in order to get the total uncertainty we show on the laboratory results. This will be further explored in the next section where we will analyse the results of the algorithm on real aerosol filter samples and real detector from our laboratory.

4. Results on real aerosol filter sample

In this section, we show the results of the unmixing on real aerosol filter sample. We show that it performs very well on this sample, allowing to detect a few Bq of ^{123}I with a correct uncertainty after only a few minutes of measurement. After the spectral signatures have been calibrated in energy and resolution to fit the observed spectrum we can estimate the activities of the 12 radionuclides of interest. The number of channels of the spectra is $C = 27\ 000$ going from 30 keV to 2 730 keV.

The results of the algorithm are presented in figure 7. This figure presents the activity estimation of the same radionuclides we showed in the simulations as they are representative of each group of radionuclides of interest. These estimations are obtained using every new elements we presented in the past section. We have adopted a buffer of size 5 thus reducing the size of the matrix. We have chosen $\beta = 2$ as seen in section 3 so that we reduce the number of iterations while keeping a correct activity estimation. Finally we chose to stop the update of the radionuclide if their expected number of counts was lower than 10 in the whole spectrum. The total number of segments is 355, we chose to have a duration of 2 minutes for the first segment and to keep the same number of counts for every time segment (each time segment thus having ~ 26000 counts).

As we can see in figure 7 the estimation of every radionuclide is quick. Indeed except for ^{137}Cs the estimation is stable after only 20-30 minutes of measurement. The new algorithm allows us to estimate the activities as soon as possible and to cope with a large number of spectra, which was impossible with the first version of the data processing. This allows to detect ^{123}I as soon as 2 minutes after the measurement started. This radionuclide is not usually observed in the environment and shows the interest of our method for the early detection of contamination. Indeed if the routine methods was used, observing a decay period before the measurement starts and only estimate the activities after the week-long measurement the contamination by ^{123}I would have been missed or given very late. These results show the performances of our new algorithm as

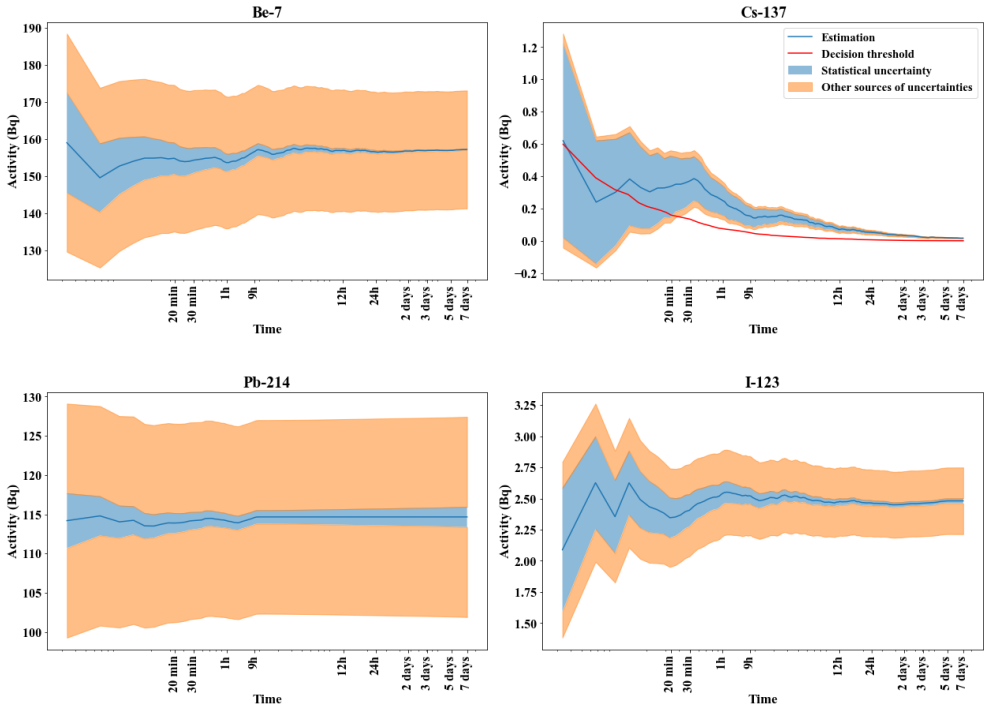

Figure 7: The results of the activity estimation on real aerosol filter samples for ^{7}Be, ^{137}Cs, ^{214}Pb and ^{123}I. The statistical uncertainties are computed following Xu et al. (2022b) and the metrological uncertainties represent 10% of the estimated activities.

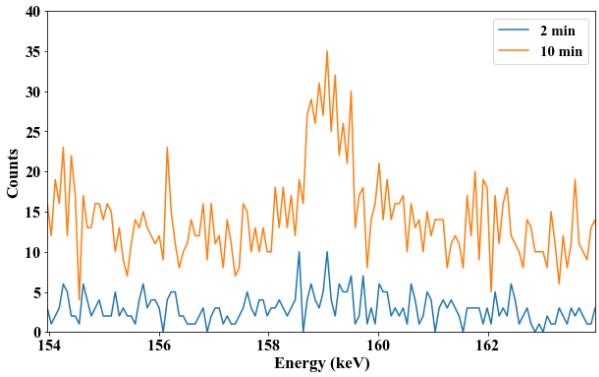

Figure 8: The cumulative spectrum of the peak region of the ^{123}I, we can see that the peak growing as the measurement proceeds. We can note that the first estimations are based on a really low number of counts showing the performances of the unmixing.

it is able to detect contamination out of a very complex spectrum in a very short time and with an algorithm that is fast to compute and reliable. Figure 8 presents the peak of interest of ^{123}I at the beginning of the measurement, showing how minute it is in the first segments. The algorithm is still able to detect the radionuclide and to estimate its activity correctly.

The estimation of ^{137}Cs is the hardest of the 12 radionuclides we are focusing on in this paper, as it is at very low level (only a few mBq) it is the only one where the estimated activity is of the same order of magnitude as the decision threshold. We saw in the simulations that the correct estimation can be late if the level is too low (0.01 Bq in the simulation). In the aerosol filter sample we analysed it seems that the activity of ^{137}Cs is high enough so that the detection is achieved after 20 minutes. But we can see a bias between the estimation on the first few time segments (0.4-0.6 Bq) and the final estimation (0.02 Bq). The estimation of radionuclides that are at the level of the decision threshold is always problematic and the results must be given within the correct uncertainties.

The statistical uncertainties are computed via the Fisher information as advocated in Xu et al. (2022b). The metrological uncertainties are composed of a few different factors summing to about 10% of the estimated activity, namely,

the slight variation of the geometry of the sample, its placement on the endcap of the detector, the efficiency calibration of the detector. The contributions of these factors have been characterized empirically and are the standard uncertainties used in the laboratory.. To obtain the decision threshold for a given radionuclide n, we compute simulations with its simulated activity equal to $0(a_n = 0$ in equation 6) and take the quantile of the activity estimation corresponding to the α risk that we want (here $\alpha = 5\%$ is taken).

5. Conclusion and perspectives

In this paper, we introduce an online spectral unmixing algorithm which allows achieving radionuclide activity estimation from temporal gamma spectroscopy measurements. Following Malfrait et al. (2023). accounting for time information in the unmixing procedure provides early estimation of the radionuclides composing the spectra earlier in the measurement process at the cost of large uncertainties at the beginning of the measurement reducing as the measurement processes. Time segmentation allows taking into account the time correlation in the unmixing algorithm and thus reduce the uncertainties and allows to deal with short-lived radionuclides such as the radon progeny. However, processing measurements with increasingly shorter time segments entails cumbersome computation issues if the algorithm is not adapted to a large number of time segments. To alleviate this bottleneck, the solutions we propose allows to reduce the number of iteration of the algorithm we presented in Malfrait et al. (2023) and allows adapting the loss function so that the activity estimation at time $s-1$ is used at time s as a guideline so that the new estimation is not too far from the precedent one. The results on real aerosol filter samples show that contaminations with a few Bq of ^{123}I can be correctly estimated after a few minutes of measurement. This could not have been achieved in the routine measurement scheme where a decay period of 2-4 days is observed so that the radon progeny decay and the spectrum simplifies.

Appendix A. Detector

The HPGe detector used in this paper is a Broad Energy Germanium detector (BEGe5030, Mirion-Canberra). Its resolution is 0.5 keV at 59 keV, 1.2 keV at 662 keV and 1.8 keV at 1332 keV. Its relative efficiency is 51%. This setup is used to measure aerosol filter collected by a high volume air sampler (700-900 m^3/h). The 45 x 45 cm^2 filters are compressed into standard 10 mL cylindrical geometries (dimensions: $\emptyset = 52$mm, $h = 4.7$mm). The detector is placed in the shallow shielded room in the second basement of the laboratory under 3 meters of borated concrete to reduce the cosmic ray induced background. This $20m^2$ room is made of 10cm thick lead bricks internally covered by 5mm copper - so that the telluric radioactive background is reduced by 2 orders of magnitude. The detector is connected to a digital electronics (Pixie-4, XIA) allowing us to proceed the data in list mode. This acquisition mode provides a list of all the detected events with time stamps and channel allowing us to separate the whole acquisition into time segments of the duration we chose.

The background spectrum is considered to be constant throughout the measurement. It is measured with the empty detector during a week and standardized to a second by dividing the intensity of each channel by the duration of the measurement. The background measurement has been measured a few weeks before the aerosol filter measurement so that it is very close to the real background during the sample measurement.

References

André, R., Bobin, C., Bobin, J., Xu, J., de Vismes Ott, A., 2020. Metrological approach of gamma-emitting radionuclides identification at low statistics: application of sparse spectral unmixing to scintillation detectors. Metrologia URL: http://iopscience.iop.org/article/10.1088/1681-7575/abcc06.

Berlizov, A., 2012. A Correlated Particle Source xtension of a General Purpose Monte Carlo N-particle Transport Code MCNP-CP Upgrade Patch Version 3.2.

Chaouai, Z., Daniel, G., Martinez, J.M., Limousin, O., Benoit-Lévy, A., 2022. Application of adversarial learning for identification of radionuclides in gamma-ray spectra. Nuclear Instruments and Methods in Physics Research Section A: Accelerators, Spectrometers, Detectors and Associated Equipment 1033, 166670. URL: https://www.sciencedirect.com/science/article/pii/S0168900222002248, doi:https://doi.org/10.1016/j.nima.2022.166670.

de Oliveira, F., Daniel, G., Limousin, O., 2023. Artificial gamma ray spectra simulation using generative adversarial networks (GANs) and supervised generative networks (sgns). Nuclear Instruments and Methods in Physics Research Section A: Accelerators, Spectrometers, Detectors and Associated Equipment 1047, 167795. URL: https://www.sciencedirect.com/science/article/pii/S0168900222010877, doi:https://doi.org/10.1016/j.nima.2022.167795.

Gilmore, G., 2001. Practical Gamma-ray Spectrometry. Second ed., Wiley-Blackwell.

Hendriks, P., Limburg, J., de Meijer, R., 2001. Full-spectrum analysis of natural γ-ray spectra. Journal of Environmental Radioactivity 53, 365–380. doi:10.1016/S0265-931X(00)00142-9.

Kirkpatrick, J.M., Young, B.M., 2009. Poisson statistical methods for the analysis of low-count gamma spectra. IEEE Transactions on Nuclear Science 56, 1278–1282. doi:10.1109/TNS.2009.2020516.

Knoll, G.F., 2010. Radiation Detection and Measurement. 4th ed., John Wiley & Sons.

Kullback, S., Leibler, R.A., 1951. On Information and Sufficiency. The Annals of Mathematical Statistics 22, 79 – 86. doi:10.1214/aoms/1177729694.

Lee, D.D., Seung, H.S., 1999. Learning the parts of objects by non-negative matrix factorization. Nature 401, 788–791.

Malfrait, P., Bobin, J., de Vismes Ott, A., 2023. Spectral unmixing of multi-temporal data in gamma-ray spectrometry. Nuclear Instruments and Methods in Physics Research Section A: Accelerators, Spectrometers, Detectors and Associated Equipment 1045, 167547.

Mirion-Canberra, 2016. Genie 2000. URL: https://www.mirion.com/products/genie-2000-gamma-analysis-software.

Paradis, H., de Vismes Ott, A., Cagnat, X., Piquemal, F., Gurriaran, R., 2017. Leda: A gamma-gamma coincidence spectrometer for the measurement of environment samples. Applied Radiation and Isotopes 126, 179–184. URL: https://www.sciencedirect.com/science/article/pii/S0969804316304377, doi:https://doi.org/10.1016/j.apradiso.2016.12.049. proceedings of the 7th International Conference on Radionuclide Metrology – Low-Level Radioactivity Measurement Techniques.

Turner, A., Wheldon, C., Kokalova, W.T., Gilbert, M., Packer, L., Burns, J., Freer, M., 2021. Convolutional neural networks for challenges in automated nuclide identification. Sensors (Basel) 21, 5238. doi:https://doi.org/10.3390/s21155238.

Xu, J., Bobin, J., de Vismes Ott, A., Bobin, C., 2020. Sparse spectral unmixing for activity estimation in γ-ray spectrometry applied to environmental measurements. Applied Radiation and Isotopes 156, 108903.

Xu, J., Bobin, J., de Vismes Ott, A., Bobin, C., Malfrait, P., 2022a. Analysis of gamma-ray spectra with spectral unmixing, part 1: Determination of the characteristic limits (decision threshold and statistical uncertainty) for measurements of environmental aerosol filters. Applied Radiation and Isotopes 182, 110109.

Xu, J., Bobin, J., de Vismes Ott, A., Bobin, C., Malfrait, P., 2022b. Analysis of gamma-ray spectra with spectral unmixing, part 2: Recalibration for the quantitative analysis of HPGe measurements. Applied Radiation and Isotopes 182, 110082.